Symmetry of pairing states in cuprate superconductors

Yueqing Chang

Abstract

Ever since the discovery of the high-T_c cuprate superconductors in 1986, physicists have been endeavoring to understand the pairing mechanism of these unconventional superconducting materials. Non-phase-sensitive and phase-sensitive experiments show strong evidences for the d-wave pairing in cuprates, either via measurement of the penetration depth in low temperature regime, and determination of the modulation pattern of critical currents with respect to external field. In this essay, we include a discussion about the symmetry of the unconventional pairing states in cuprates and review the early experimental efforts in establishing their d-wave symmetry.

1 Introduction

Since the discovery of the high-T_c cuprates ($La_{2-x}Ba_xCuO_4$) in 1986 by Bednorz and Müller, physicists have been trying to understand the mechanism of superconducting in these materials. In superconductors, fermionic electrons form Cooper pairs, which consist of electrons with opposite momenta, and behave as effective bosons. Thus they can form superconducting state analagous to the Bose-Einstein condensate. The collective manner exhibited by these pairing states give rise to the Meissner effect, i.e., superconductors expel magnetic fields.

The pairing mechanism for conventional superconctors are well established so far, within the context of the Bardeen, Cooper, and Schrieffer (BCS) theory (1957). Since the fermionic wave functions are antisymmetric under exchange of any pair of electrons, the pairing state in superconductor should also have such property. Thus, if the spin part of the pairing state is spin singlet ($s = 0$), which is antisymmetric under exchange of electrons, then the spatial part should have even parity. It turns out that the spin singlet pairing state with s-wave spatial component forms the pairing wave function in conventional superconductors. The pairing is mediated by phonons, which can be interpreted as arising from the fact that ions have much slower response relative to the electrons. Thus, when an electron attracts the surrounding ions and induces a geometric distortion, it will attract a second electron effectively, leading to a net attraction between electrons.

However, this picture does not apply to cuprates. Cuprates are complicated materials that may exhibit charge density waves, spin-density waves, nematic correlations and orbital currents at low temperatures, all of which may play important roles in forming superconducting state [1]. In order to understand the true mechanism behind high-T_c superconducting states in cuprates, the first step is to determine the symmetry of its pairing state.

Non-phase-sensitive experimental techniques, including measurements of the penetration depth measurements, determination of the gap function using angl-resolved photoemission spectroscopy (ARPES), Raman scattering and nuclear magnetic resonance (NMR), suggest that the gap function have nodes on Fermi surface and change its sign there. These nodes may be at the same positions with the nodes of $d_{x^2-y^2}$ state [2, 3]. Phase-sensitive tests, including the two-junction interferometer (dc SQUID) experiment, and the modified single-junction modulation experiment, lead to the conclusion that the pairing states in cuprates take $d_{x^2-y^2}$ symmetry [4]. In this review, we focus on these two types of experiments: the penetration depth measurements and the dc SQUID experiment performed on $YBa_2Cu_3O_{7-\delta}$ (YBCO). Hopefully, this will motivate the further studies about the superconducting mechanism in cuprates.

2 Mixing of different symmetries

Here we review the discussion about the symmetry of cuprates pairing states, presented in [2]. Assume that there exists the Ginzberg-Laudau equal time order parameter for superconductor as $\Psi(\mathbf{r}_1, \mathbf{r}_2; \alpha\beta) = \langle \psi_\alpha(\mathbf{r}_1, t_1)\psi_\beta(\mathbf{r}_2, t_2)\rangle$, where $t_1 = t_2$.

If the order parameter is a superposition of two functions from different irreducible representations of the crystal symmetry group and symmetry considerations forbid "mixing" of these functions in the free energy, then *there must inevitably be a second phase transitionat some temperature below* T_c [2].

For a crystal with symmetry group $G = U(1) \otimes T_l \otimes H$, where $U(1)$ is the gauge group, T_l and H are the crystal lattice group and the crystal point group respectively, we can always expand its order parameter using the irreducible representations of group G, $\Psi(\mathbf{r}_1, \mathbf{r}_2; \alpha\beta) = \sum_l \sum_{m=0}^{D_l} \psi_{lm}\chi_{lm}(\mathbf{r}_1, \mathbf{r}_2; \alpha\beta)$, where D_l is the dimension of the l-th irreducible representation [2]. (Notes: this order parameter may be naïvely thought of as the pairing wave function)

Thus, one can write down the Ginzberg-Landau free energy in terms of the order parameter up to the fourth order. For the tetragonal and orthorhombic symmetry groups (which are the symmetry groups of the CuO_2 planes in YBCO), the "mixing" quartic terms are absent. If we only include the terms involving less than 3 distinct representations and ignore higher order terms [2],

$$\begin{aligned} F(T) &= \sum_{lm} \left(\alpha_l(T) \left|\psi_{lm}\right|^2 + \frac{1}{2}\beta_{lm_1m_2m_3m_4}\psi^*_{lm_1}\psi_{lm_2}\psi_{lm_3}\psi_{lm_4} \right) \\ &= + \sum_{l_1,l_2,m_1,m_2,m_3,m_4} \frac{1}{2}\beta_{l_1l_2m_1m_2m_3m_4}\psi^*_{l_1m_1}\psi_{l_1m_1}\psi^*_{l_2m_3}\psi_{l_2m_4} \\ &\quad + \sum_{l_1,l_2,m_1,m_2,m_3,m_4} \frac{1}{2}\kappa_{l_1l_2m_1m_2m_3m_4}\psi^*_{l_1m_1}\psi^*_{l_1m_2}\psi_{l_2m_3}\psi_{l_2m_4} \end{aligned} \tag{1}$$

At sufficiently high temperature, all $\alpha(T)$s are positive, the minimum $F(T)$ occurs when all ψ_{lm} vanish, i.e., the system is in normal state. As the temperature decreases to slightly below $T_c^{l_0}$, which corresponds α_{l_0} first becomes negative and all the other α_ls remain positive, if l_0 representation is multidimensional, some or all of the ψ_{l_0m} will be nonzero. A more relevant case to high-T_c superconductor is that the irreducible representation l_0 is one-dimensional. We are interested in the condition that below $T_c^{l_0}$, some ψ_{lm} corresponds to other values of l are nonzero (i.e., there is mixing between different symmetries). Without loss of generality, assume $l_0 = 1$ and only one relevant irreducible representation 2 besides l_0 and it is also one-dimensional, then we can always minimize the free energy by choosing $\arg(\psi_{l_0m_0}\psi_{lm})$ to be either 0 or π [2].

$$\begin{aligned} &F(T) = F_0(T) + \alpha_1(T)|\psi_1|^2 + \alpha_2(T)|\psi_2|^2 + \frac{1}{2}\beta_1(T)|\psi_1|^4 + \frac{1}{2}\beta_2(T)|\psi_2|^4 + \kappa(T)|\psi_1|^2 \cdot |\psi_2|^2 \\ &\alpha_1(T) = \alpha_1(T - T_{c_1}),\ \alpha_2(T) = \alpha_2(T - T_{c_2}),\ T_{c_2} \le T_{c_1},\ \beta_1(T) = b_1,\ \beta_2(T) = b_2,\ \kappa(T) = \kappa \end{aligned} \tag{2}$$

Stability requires $\beta_1, \beta_2 > 0$, $\kappa > -\sqrt{\beta_1\beta_2}$. When temperature is above T_{c_1}, $\psi_1 = \psi_2 = 0$ (normal phase). For T just below T_{c_1}, $F(T)$ is minimized by the choice [2],

$$\psi_1 = \frac{\alpha_1}{\beta_1}(T_{c_1} - T)^{1/2}, \quad \psi_2 = 0 \tag{3}$$

If ψ_2 is ever to become nonzero, either it must jump discontinously from zero to this value (which corresponds to a first order transition), or there must be a second second order transition at T^* such that $T^* - T_{c_2} = \lambda(T^* - T_{c_1})$, $\lambda = \kappa\alpha_1/\alpha_2\beta_1$. One can show that there is a discontinuity in the specific heat at T^*. Also, many other physical quantities (e.g., the mean-square energy gap) will be roughly proportional to the change in the slope at T^* of the total order parameter, unless T_{c_2} is very close to T_{c_1}. Thus, one can draw the conclusion: *If the order parameter is a superposition of two functions from different irreducible representations of the crystal symmetry group, and symmetry considerations forbit the mixing of these two functions, then there must be a second phase transition at some temperature below* T_c [2].

For some high-T_c superconductors, where there is orthorhombic anisotropy, small but nonzero mixings between states from different irreducible representations are allowed. One can also show that a second phase transition below $T_c^{l_0}$ is neccessary for a mixed symmetry state to exist at low temperature [2].

3 Candidates for the pairing state

The high-temperature cuprates, either tetragonal or orthorhombic, are highly anisotropic materials that have a layered structure. The superconductivity is believed to occur in the CuO_2 planes, which is in a square lattice in tetragonal case (Hg-1201 and $Tl_2Ba_2CuO_{6+\delta}$ (Tl-2201), etc.) and is in rectangular lattice in the orthorhombic case (YBCO and $Bi_2Sr_2CaCu_2O_8$ (Bi-2212), etc.) [3].

The measurement of the temperature dependence of the NMR relaxation rates provides evidence for the spin-singlet pairing [5]. Thus, one can use Pauli exclusion to exclude odd parity in the spatial part of the pairing state, i.e., it can only be s, d, g, etc.. Theoretical studies establish the spin fluctuation model and verify that it can promote pairing in a $d_{x^2-y^2}$ channel [4]. However, with so many proposed candidates, the pairing symmetry remains to be experimentally validated.

Follows are the band gap $\Delta(\mathbf{k})$ of candidate pairing states, along with diagramatic representations of their magnitudes and phases (shown in Fig. 1, left panel):

The conventional superconducting state has symmetry s, which gives rise to an isotropic band gap. $d_{x^2-y^2}$ pairing state leads to nodes in magnitude and discontinuities in phase along the (110) directions [4].

$$[d_{x^2-y^2}] \quad \Delta(\mathbf{k}) = \Delta_0 \left[\cos(k_x a) - \cos(k_y a)\right] \tag{4}$$

The anisotropic s state has only attenuations in magnitude of $\Delta(\mathbf{k})$ along (110), but shows no discontinuities in its phase. Δ^1 denotes the minimum value of the gap, which occurs along the diagonal directions.

$$[\text{ anisotropic } s] \quad \Delta(\mathbf{k}) = \Delta_0 \left[\cos(k_x a) - \cos(k_y a)\right]^4 + \Delta_1 \tag{5}$$

The extended s does have jumps in phase. However, the nodes in magnitude are shifted away from diagonal directions due to the nonzero γ^2 term.

$$[\text{ extended } s \text{ wave }] \quad \Delta(\mathbf{k}) = \Delta_0 \left\{(1+\gamma^2)\left[\cos(k_x a) - \cos(k_y a)\right]^2 - \gamma^2\right\} \tag{6}$$

The mixed pairing states $s + id_{x^2-y^2}$ and $d_{x^2-y^2} + id_{xy}$ are also allowed by symmetry. Like the anisotropic s state, they also do not show vanishing band gap but only attenuation along the diagonal. Also, their phases are continuously varying.

$$[s + id] \quad \Delta(\mathbf{k}) = \Delta_0 \left\{\epsilon + i(1-\epsilon)[\cos(k_x a) - \cos(k_y a)]\right\} \tag{7}$$

$$[d+id] \quad \Delta(\mathbf{k}) = \Delta_0 \left\{(1-\epsilon)[\cos(k_x a) - \cos(k_y a)] + i\epsilon[2\sin(k_x a)\sin(k_y a)]\right\} \tag{8}$$

In order to determine which one is the true pairing state in cuprates, one needs to measure the anisotropy of the order parameter $\Delta(\mathbf{k})$. Most experiments, including angle-resolved photoemission, NMR spectroscopy, scanning tunneling microscopy, thermal conductivity in a magnetic field, and measurement of the low-temperature penetration depth, are sensitive only on the magnitudes of Δ. In section 3, we will introduce the details and results of the low-temperature penetration depth measurement which establishes the anisotropy of the gap magnitude based on the power law dependence at low temperature [4].

From Fig. 3 we see that the phases for s-wave states and d-wave states are distinctly different in a sense that s-wave states exhibit uniform phase, while d-wave states show discontinuous jumps at (110) lines. The mixed states, $s+id$ and $d+id$, have continuous varying phases. Therefore, it will be ideal if one can design experiments that can probe the phase changes in particular directions. We will introduce the phase sensitive experiments based on superconducting quantum interference device (SQUID) which involves two-junction interference and the single-junction modulation experiment in section 5.

4 Measurement of the low-temperature dependence of the penetration depth in $a-b$ plane

The electromagnetic penetration depth directly reflects the response of the condensate to electromagnetic perturbations, and thus is a measure of the superfluid density tensor. The asymptotically low temperature regime can directly test the changes in sign of the gap function over the Fermi surface. Different varieties of nodal structure, which is related to the pairing state symmetry, give rise to different power low dependence of the $\Delta\lambda_{a,b}$ when $T \to 0$ [2]. With orthorhombic crystal symmetry, the conventional $s-$wave pairing will give rise to a cubic dependence in low temperature regime, while singlet pairings other than s-wave pairing gives rise to linear dependence. This can be used to rule out candidates of conventional pairing states, since linear dependence is easier to be discerned comparing with the cubic dependence [6].

4.1 Theoretical framework

The temperature dependence of the electromagnetic penetration depth λ at low temperature is a potential probe of the pairing state symmetry in superconductors. In a perfect orthorhombic crystal, the penetration depth tensor λ has three components in the three directions. Here we consider the measurement of the component lying in the $a-b$ plane [6].

The unconventional singlet state, e.g. d-state, gives rise to the following linear temperature dependence for $\lambda_a(T)$, and cubic dependence for $\lambda_b(T)$ [6]

$$\frac{\Delta\lambda_a(T)}{\lambda_a(0)} \approx A\left(\frac{T}{T_c}\right) + O\left(\left(\frac{T}{T_c}\right)^2\right), \quad \frac{\Delta\lambda_b(T)}{\lambda_b(0)} \approx C\left(\frac{T}{T_c}\right)^3 + O\left(\left(\frac{T}{T_c}\right)^4\right) \tag{9}$$

where $\Delta\lambda_a \equiv \lambda_a(T) - \lambda_a(0)$.

It is impossible to determine the pairing state from the temperature dependence away from the low temperature regime due to the interplay of strong-coupling corrections, dirt, the precise shape of Fermi surface and gap anisotropy etc.. One cannot conclude that pairing state is s-wave simply by fitting the result to the BCS result, because many other pairing symmetries lead to the similar looking temperature dependence away from the low temperature regime [6].

The quantities $\Delta\lambda_a(T)$ and $\Delta\lambda_b(T)$ are proportional to a and b diagonal components of the normal fluid density tensor, ρ^n_{ij}, which is given by [6]

$$\rho^n_{ij} = \frac{m}{\hbar}\int \frac{d^2k}{(2\pi)^3|\mathbf{v}|} v_i v_j \int d\epsilon_k \frac{\beta}{2}\mathrm{sech}^2\left(\frac{\beta E_k}{2}\right) \tag{10}$$

where $\beta =\equiv 1/(k_B T)$, and ϵ_k is the normal state band energy, $E_k = \sqrt{\epsilon_k^2 + |\Delta_k|^2}$ is the quasiparticle energy. If the excitation gap Δ_k closes on lines on the Fermi surface, one can see that some components of ρ^n vanishes linearly with T, i.e., if there are a line of nodes on plane $k_z = 0$, we have $\rho^n_{ij} \propto \mathrm{diag}(I^x_0\eta, I^y_0\eta, I^z_2\eta^3)$, where $\eta = k_B T/\Delta_{\max}$ is the maximum of the zero temperature energy gap over the Fermi surface. If there are four line of nodes parallel to the c axis, for example, $k_x = 0$ and $k_y = 0$, we have $\rho^n_{ij} \propto \mathrm{diag}\left(I^x_0\eta + I^x_2\eta^3, I^y_0\eta + I^y_2\eta^3, I^z_0\eta\right)$. Thus, for all possible single pairing other than the s-wave symmetry, both $\Delta\lambda_a(T)$ and $\Delta\lambda_b(T)$ scale **linearly** with T in the low temperature regime [6].

In practice, due to the presence of crystal twinning, one measures the averaged $\Delta\lambda_{ab}$ over the ab plane. One may conclude that after performing the averaging, $\Delta\lambda_{ab}(T) \propto T$ as $T \to 0$. Thus, if a linear dependence is not observed, the pairing states with line nodes in orthorhombic or tetragonal crystals can be ruled out. The only states permitted would be s-wave or those with point nodes [6].

4.2 Results and analysis

The data from [7] is reanalyzed in ref [6]. In reference [7], Fiory *et al.* measure the surface impedance of two epitaxial thin films of thickness 500 and 200 Å. λ_{ab} is calculated using $L = \frac{4\pi}{c^2}\frac{\lambda^2_{ab}}{d}$, where L is the inductive component. The results are fitted to BCS theory and $\lambda_{ab} = 1500$ Å and 2100 Å are found. This discrepancy is attributed to the Josephson coupling between the grains in the thicker film [6].

It is pointed out that fomula used to extract λ_{ab} is not valid in the $d = 2000$ Å regime. The complete expression should be given by solving the Maxwell's equations for electromagnetic waves incident on a free standing slab of superconductor: $L = \frac{4\pi}{c^2}\lambda_{ab}\coth\left(\frac{d}{\lambda_{ab}}\right)$.

The measured λ_{ab} versus temperature is replotted on an expanded scale, shown in Fig. 1. The left panel shows an upward curvature at even the lowest temperatures. The linear dependence $\frac{\Delta\lambda_{ab}(T)}{\lambda_{ab}(0)} = A\left(\frac{T}{T_c}\right) + O\left(\left(\frac{T}{T_c}\right)^2\right)$ is assumed when fitting the coefficient A. A lies between 0 and 0.13 for the thinner film and between 0 and 0.21 forr the thicker film [7].

The right panel shows the same data, replotted as λ_{ab} versus T^2 in the lower temperature region. The clear linear dependence suggests that the data is better described by the model $\frac{\Delta\lambda_{ab}(T)}{\lambda_{ab}(0)} = B\left(\frac{T}{T_c}\right)^2 + O\left(\left(\frac{T}{T_c}\right)^3\right)$ instead of the BCS prediction. The coefficient B is estimated to

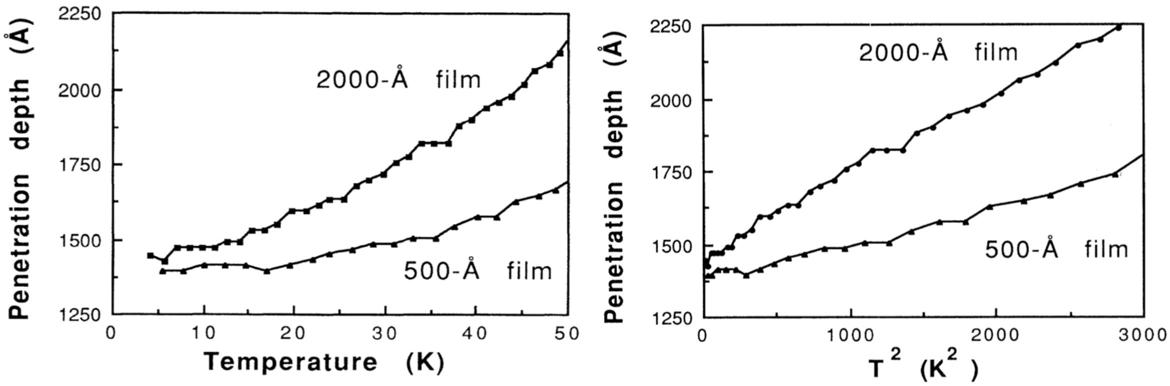

Figure 1: Reprinted from [6]. Left panel: Data extrated from [7], replotted as $\Delta\lambda_{ab}$ vs. T in the low temperature regime. Right panel: The same data, but replotted as $\Delta\lambda_{ab}$ vs. T^2.

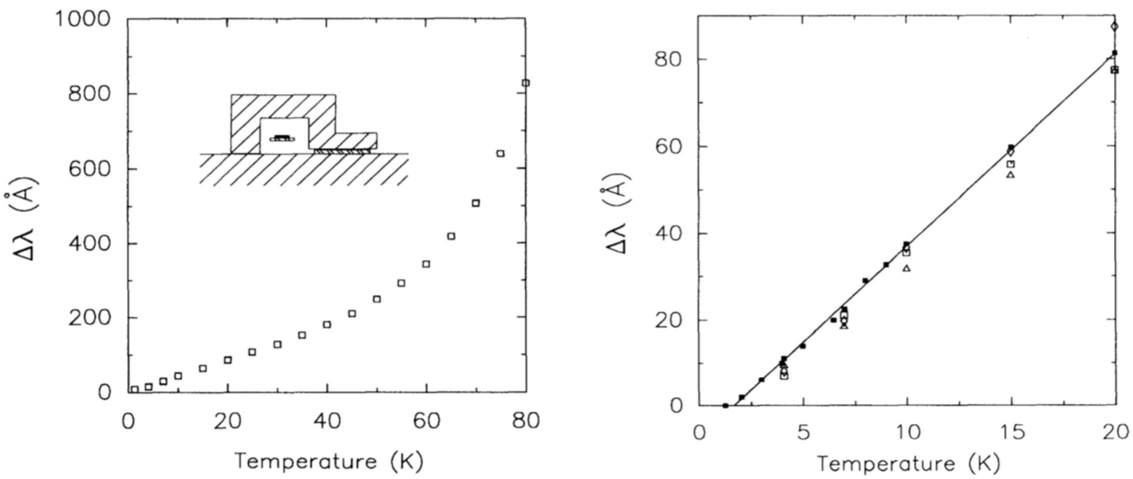

Figure 2: Reprinted from [8]. Left panel: $ab-$plane averaged penetration depth $\Delta\lambda_{ab}$ vs. T on a larger temperature scale. Right panel: $\Delta\lambda_{ab}$ vs. T, zoomed in to the low temperature limit.

be 0.63 for thinner film, and 1.6 for the thicker film. The sample dependence of B is attributed to nonmagnetic impurity scattering, which is sample dependent [6].

Therefore, the reinterpretation of the data in low-temperature regime as $\Delta\lambda_{ab} \propto T^2$ is inconsistent with the exponential temperature dependence, but consistentwith unconventional singlet state subject to impurity scattering.

The follow-up work includes accurate and controlled measurements on very clean YBCO single crystals, which indicate a strong linear temperature dependence of the penetration depth in low temperature regime. Those results clearly rule out the much weaker dependence expected for a nodeless superconductor [8].

From the experimental measurements of low-temperature asymptotic behavior of the ab-plane penetration depth, we see the strong linear dependence is clearly different from that in any conventional $s-$wave pairing. This is within the context of the orthorhombic (or near tetragonal) symmetry, where conventional singlet pairing will give rise to linear dependence for both λ_a and λ_b at low temperatures.

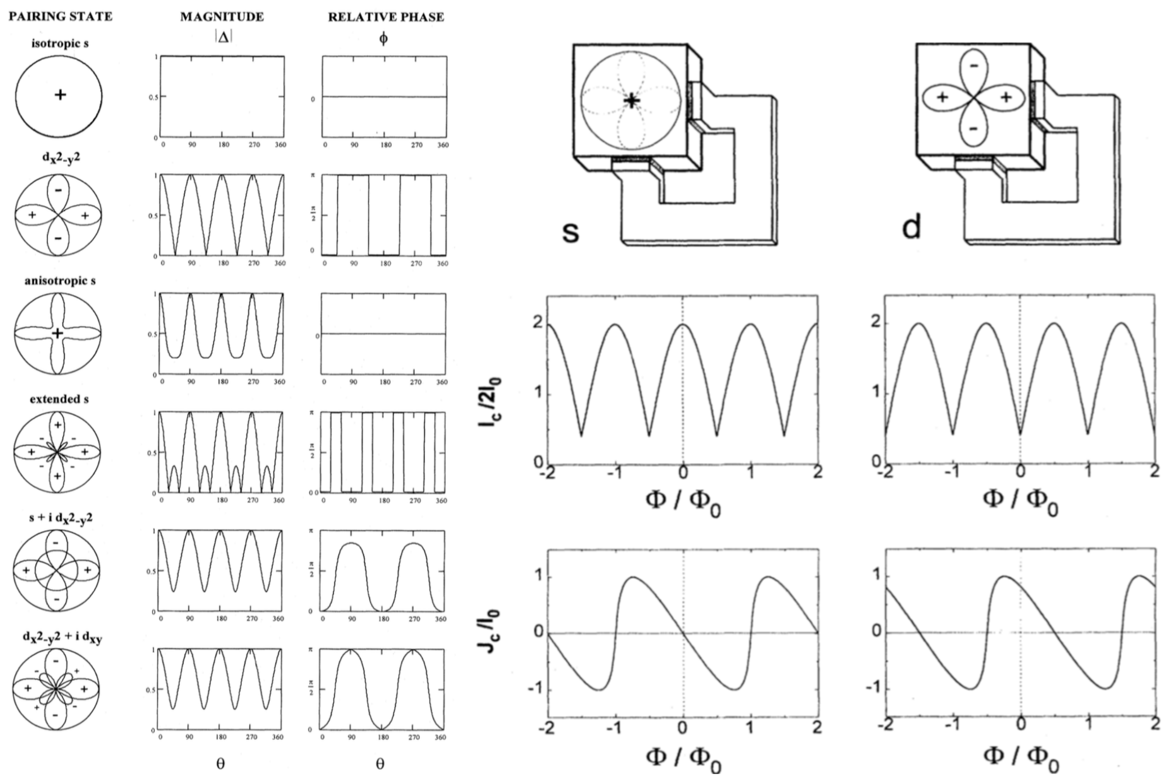

Figure 3: Reprinted from [4]. Left panel: Predictions of the pairing states in YBCO, and corresponding spatial distributions of their magnitudes and relative phases. Right panel: Experimental setup of the corner SQUID. Modulation of the critical current and circulating supercurrent vs. applied magnetic flux if the pairing state is s-wave or $d-$wave symmetry.

5 Phase-sensitive tests about pairing states

5.1 Two-junction interferometer (dc SQUID)

The two-junction interferometer (dc SQUID) experiment determines the symmetry of pairing state inside YBCO crystal based on observing the modulation of response versus the applied magnetic flux and thus determining the phase shift between pairs tunneling in two perpendicular directions. The experiment is designed based on the following ideas [4]:

- The dc Josephson effect describes the dc current flowing between two superconductors due to the phase difference between them, without any applied voltage. The supercurrent in a Josephson junction depends on the phase difference ϕ according to $I = I_c \sin\phi$, where I_c is the critical current dependent on the gap function. The experiment utilizes the interference between the supercurrents inside two Josephson junctions attached to different faces of one crystal to determine the gauge-invariant phase difference across the junctions on different faces of the crystal [4].

- Two superconductors and two junctions form a connected loop around which the phase coherence of the superconducting state is maintained. This is to make sure that the condensate wave function is single valued so that it is sensitive to intrinsic phase shifts within the superconductors arising from the symmetry of the pairing interactions [4].

5.1.1 Theoretical framework

The experiment setup includes two configurations of SQUIDs based on Josephson junctions attached to YBCO crystal: the coner SQUID (shown in figure 3), which is used to determine the relative phase between orthogonal direction, and the edge SQUID (not shown here), which is used as a control sample. In the coner SQUID interferometer, with junction critical currents I_{ca} and I_{cb}, and an applied bias current I: $I = I_{ca}\sin\phi_a + I_{cb}\sin\phi_b$. Phases ϕ_a and ϕ_b satisfy the constraint [4]

$$\phi_a - \phi_b + 2\pi\left(\frac{\Phi}{\Phi_0}\right) + \delta_{ab} = 0 \tag{11}$$

where $\Phi = \Phi_{\text{ext}} + LJ$ is the magnetic flux inside the loop including the contribution from circulating current J and self-inductance L. δ_{ab} is the intrinsic phase shift inside the YBCO between the Cooper pairs tunneling in the a and b directions. If the pairing state is of s or $d+id$ symmetry, $\delta_{ab} = 0$. $\delta_{ab} = \pi$ for $d_{x^2-y^2}$ pairing state, and $(1-\epsilon)\pi$ for $s+id$ mixture with ϵ the fraction of s-wave component. For a symmetric dc SQUID, $I_{ca} = I_{cb} = I_0$, thus

$$I_c(\Phi_{\text{ext}}) = 2I_0\left|\cos\left[\pi\frac{\Phi_{\text{ext}}}{\Phi} + \delta_{ab}\right]\right| \tag{12}$$

Now consider the corner SQUID configuration. If the pairing state inside YBCO has s-wave symmetry with isotropic phase, the phase of the order parameter is the same at each junction inside YBCO, i.e., $\delta_{ab} = 0$, then maximum of critical current occurs at zero Φ_{ext}, and the circulating current $J_0 = 0$ at this point. If the pairing state is of anistropic $d_{x^2-y^2}$ symmetry, the intrinsic phase shift $\delta_{ab} = \pi$ will shift the maximum of I_c. At zero external flux, two junction currents are exactly out of phase, thus the critical current I_c is minimum. Meanwhile, a finite circulating current must flow across the loop in order to maintain the phase coherence . If the pairing state has $s+id$ symmetry, the phase shift is between 0 and π determined by the fraction of s in the mixed state. Thus, one can determine the symmetry by observing the modulation of the SQUID response I_c and J_c versus Φ_{ext} [4].

5.1.2 Experimental details

In the SQUID experiment, many complicating issues, including twining, asymmetry, residual magnetic fields, trapped flux and corners need to be addressed. Both theoretical and experimental evidence show that order parameter maintains its orientation across twin boundaries. The asymmetry of the sample will also affect the result since $I_{ca} = (1-\alpha)I_0$ may not equal $I_{cb} = (1+\alpha)I_0$, where α is the asymmetry parameter. This imbalance in currents may give rise to a net magnetic flux in the loop, thus suppressing and shifting the flux modulation pattern. Also, if the inductance of the arms of SQUID is asymmetric, it will be necessary to determine the critical current numerically in this configuration [4].

Apart from the geometry of the sample, other serious concerns include residual magnetic fields and the trapping of magnetic flux near the SQUID, both of which create a shift in the

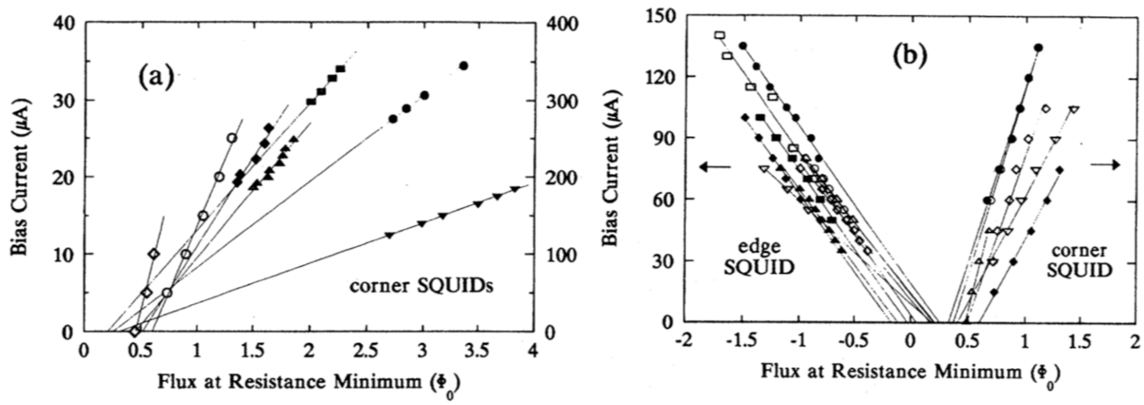

Figure 4: Reprinted from [9]. Panel (a): Minima in the SQUID modulation curves extrapolated to zero bias current for seven different samples. Zero intercept is expected for $s-$wave pairing, while $d_{x^2-y^2}$ gives rise to intercept near $\Phi_0/2$. Panel (b): Comparism of the corner SQUID and the edge SQUID on the same crystal cooled down for several times.

flux modulation pattern. They can be taken into account by reducing the ambient magnetic field and cooling the SQUIDs many times to determine the lowest-energy state which has no trapped flux [4].

Another concern is that there may be a singularity in the supercurrent flow or a difference in the probability of trapping at the corner. Experiments show that the current at even perfectly sharp corner is smooth, and flux trapped at the corner shows no difference from that at the edge. Thus, the corner plays no significant role, and the edge configured SQUID can be used as a control sample where the two currents are in phase [4].

5.1.3 Results and discussions

In the SQUID experiment conducted at UIUC, only YBCO crystals with smooth, flat, natural growth faces and a sharp corner are selected. This makes sure that the tunneling is directional and allows the probing of the order parameter anisotropy. 100-200 nm of Au is coated on to the a-c and b-c faces, and a 800 nm Pb film is deposited to define the loop and form electrical leads. The YBCO-Au-Pb junctions are superconductor-normal metal-superconductor (SNS) junctions [4].

The resistivity vs different applied magnetic flux is measured, showing the expected periodic dependence. In order to extract the instrinsic phase shift δ_{ab}, one can either use a nearly symmetric sample, or extrapolate the phase of the R vs Φ to the zero-current limit. In figure 4, the bias current vs the value of the applied flux when critical current is at maximum is plotted for many different samples. This procedure is valied in the regime near the critical current. The slopes of these fitted lines show the amounts of asymmetry in the samples [4].

Figure 4 panel (a) shows that, despite the varying amounts of asymmetry, the intercepts are $0.5\Phi_0 \pm 0.1\Phi_0$. Panel (b) shows a comparism between the results yielded by edge SQUID and corner SQUID. The intercepts given by edge SQUIDs are centered near 0, which corresponds to zero phase difference between two tunneling pairs. The $0.5\Phi_0$ intercept corresponds to a π phase shift in a and b directions, thus suggests $d_{x^2-y^2}$ pairing symmetry in YBCO. Thus, the samples studied in the SQUID experiment exhibit a significant phase shift π consistent with the $d_{x^2-y^2}$ pairing [4].

5.2 Single-junction modulation experiments

The two-junction modulation experiment applies the idea of two sources interference to measure their phase difference. However, one needs to take into account the phase shift due to the asymmetry of samples, and residue magnetic flux, etc.. One can alternatively make use of this interference idea to set up a single-junction modulation experiment, which only involves fabrication of one junction [4].

For a rectangular junction with area A, width w, magnetic barrier thickness t and uniform critical current density J_0, the critical current resembles the single-slit diffraction form [4]:

$$I_c(\phi) = J_0 A \left| \frac{\sin(\pi\Phi/\Phi_0)}{(\pi\Phi/\Phi_0)} \right|, \text{ where the total magnetic flux } \Phi = Bwt \tag{13}$$

Now consider a junction straddling the corner of a YBCO sample. If the pairing symmetry is s-wave like, the phases of pairs tunneling in perpendicular directions are the same since s-wave has uniform phase. Therefore, the relation between critical current with respect to the total magnetic flux Φ should be the same with the single junction one — resembling the Fraunhofer diffraction form. However, if the pairing in YBCO is of d-wave symmetry, the order parameters in a and b directions differ by their signs, modifying the Fraunhofer pattern. In a symmetric corner junction where a and b faces have equal geometry, the critical current modulation is given by [4]

$$I_c(\Phi) = J_0 A \left| \frac{\sin^2(\pi\Phi/2\Phi_0)}{(\pi\Phi/2\Phi_0)} \right| \tag{14}$$

which vanishes at zero applied field. The key feature to distinguish s and d-wave pairing is whether there is a dip or a peak in critical current at zero applied field.

Fig. 6 shows the results got from the single-junction modulation experiment. In panel (b), we can see a dip at zero applied flux, providing clear evidence for the d-wave pairing in the sample. The non-zero critical current at zero applied flux is due to the presence of trapped agnetic vortices, which breaks the polarity symmetry of the diffraction pattern. We can also see the shift of the pattern, which is probably due to the slight asymmetry of junctions on a and b faces [4].

To summarize, we review the two types of experiments performed on YBCO: the measurement of the temperature dependence of the averaged penetration depth in low-T regime, and phase-sensitive dc SQUID interferometer experiments.

Apart from the experiments introduced above, there are other non-phase-sensitive observations including measurement of specific heat (a line of nodes give rise to T^2 dependence), thermal conductivity (for $d-$wave gap, quasiparticle transport should be independent of the scattering rate at the limit $T \to 0$, thus thermal conductivity should be linear in T at low temperature), etc.. Experimental techiniques including angle-resolved photoemission spectroscopy (ARPES) is also used to determine the gap nodal structure directly, although hampered by its sensitivity to surface conditions. Raman scattering, which has the advantage of selecting

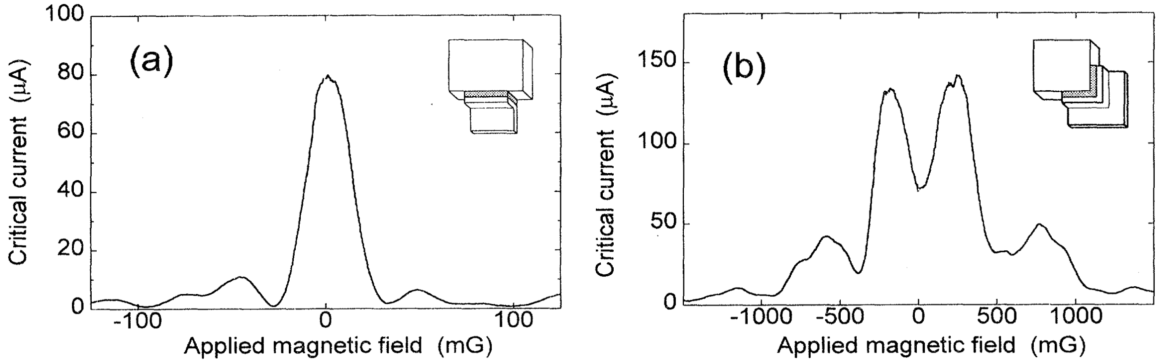

Figure 5: (Reprint from [10]) Modulation patterns measured on (a) an edge junction and (b) a corner junction. The dip at zero field flux is a strong evidence for $d-$wave pairing.

different symmetry channels from the electronic scattering spectra,is also used to determine the gap structure in cuprates [2].

6 Outlook

From the experimental observations of the pairing state using the non-phase-sensitive and the phase-sensitive techniques, the d-wave pairing for cuprates is well established. However, the detailed pairing mechanism remains unknown.

Philip Anderson proposes the resonating valence bound (RVB) state for cuprates, i.e., cuprates exhibit a novel phase of matter where the spin form a liquid of singlets, based on tha fact that cuprates are quasi-two-dimensional, the copper ions have spin 1/2, and the parent phase is Mott insulator. The RVB state is predicted to melt the expected antiferromagnetic lattice into the spin-liquid phase. Uppon carrier doping, these singlets become charged, resulting in the superconducting state. Subsequent work found that the free energy is minimized for a d-wave state [1].

On the other hand, one should notice the large exchange interaction J in cuprates (on the order of 1400 K) can be an attractive source for pairing, since it is relevant for the more traditional spin fluctuation-based mechanism. The debate about which mechanism, the RVB or spin fluctuations, should give rise to the electron pairing in cuprates, is still unresolved [1].

Moreover, at low temperatures, the charge-density waves, spin-density waves nematic correlations, orbital currents come into play, debates about whether they help to form pairing states or not are also unresolved [1].

References

[1] M. R. Norman. The challenge of unconventional superconductivity. *Science*, 332(6026):196–200, 2011.

[2] J. F. Annett, N. Goldenfeld, and A. J. Leggett. Experimental constraints on the pairing state of the cuprate superconductors: an emerging consensus. In *Physical Properties of High Temperature Superconductors V*, pages 375–461. World Scientific, 1996.

[3] C. C. Tsuei and J. R. Kirtley. Pairing symmetry in cuprate superconductors. *Reviews of Modern Physics*, 72(4):969, 2000.

[4] D. J. Van Harlingen. Phase-sensitive tests of the symmetry of the pairing state in the high-temperature superconductorsevidence for $d_{x^2-y^2}$ symmetry. *Reviews of Modern Physics*, 67(2):515, 1995.

[5] S. E. Barrett, J. A. Martindale, D. J. Durand, C. H. Pennington, C. P. Slichter, T. A. Friedmann, J. P. Rice, and D. M. Ginsberg. Anomalous behavior of nuclear spin-lattice relaxation rates in $YBa_2Cu_3O_7$ below t_c. *Physical review letters*, 66(1):108, 1991.

[6] J. Annett, N. Goldenfeld, and S. R. Renn. Interpretation of the temperature dependence of the electromagnetic penetration depth in $YBa_2Cu_3O_{7-\delta}$. *Physical Review B*, 43(4):2778, 1991.

[7] A. T. Fiory, A. F. Hebard, P. M. Mankiewich, and R. E. Howard. Renormalization of the mean-field superconducting penetration depth in epitaxial $YBa_2Cu_3O_7$ films. *Physical review letters*, 61(12):1419, 1988.

[8] W. N. Hardy, D. A. Bonn, D. C. Morgan, R. Liang, and K. Zhang. Precision measurements of the temperature dependence of λ in $YBa_2Cu_3O_{6.95}$: strong evidence for nodes in the gap function. *Physical Review Letters*, 70(25):3999, 1993.

[9] D. A. Wollman, D. J. Van Harlingen, W. C. Lee, D. M. Ginsberg, and A. J. Leggett. Experimental determination of the superconducting pairing state in YBCO from the phase coherence of YBCO-Pb dc SQUIDs. *Physical Review Letters*, 71(13):2134, 1993.

[10] D. A. Wollman, D. J. Van Harlingen, J. Giapintzakis, and D. M. Ginsberg. Evidence for $d_{x^2-y^2}$ pairing from the magnetic field modulation of $YBa_2Cu_3O_7$-Pb josephson junctions. *Physical review letters*, 74(5):797, 1995.